

# Influence of a metal–polymer interfacial interaction on dielectric relaxation properties of polyurethane

A. Korzhenko\*, M. Tabellout, J.R. Emery

*Laboratoire de Chimie et Physique des Matériaux Polymères, Département de Physique-UFR Sciences-UMR CNRS 6515, Université du Maine, BP535, 72085 Le Mans Cedex 9, France*

Received 2 October 1998; received in revised form 5 January 1999; accepted 5 January 1999

---

## Abstract

The influence of metal–polymer interaction on dielectric relaxation properties of polyurethane (PU), prepared from poly(oxypropylene)-diol and hexamethylendiisocyanate, was investigated by means of dielectric relaxation spectroscopy in the frequency domain on the dependence of the thickness of the PU layer and electrode material (gold and steel). Strong electrostatic part of an adhesion interaction between steel substrate and PU results in changes of the  $\alpha$ -,  $\beta$ -,  $\gamma$ - and Maxwell–Wagner–Sillars relaxation of the PU, as compared to a gold substrate. The effect of the metal–polymer double layer results in the complication of the cooperative and local motions in the polymer. The influence of metal–polymer interaction on the relaxation parameters becomes pronounced at a thickness of less than 60  $\mu\text{m}$  for the steel substrate. For the gold substrate the relaxation characteristics hardly depend on the thickness. © 1999 Elsevier Science Ltd. All rights reserved.

*Keywords:* Dielectric relaxation spectroscopy; Interfacial interaction; Polymer coating

---

## 1. Introduction

Formation of an electrostatic double layer at the metal–polymer interface is an important part of the adhesion strength [1–4]. The influence of the electrostatic attraction on the adhesion is valuable when there is enough high concentration of charge carriers, at least 1% per monolayer [5].

Magnitude of the electric field of the double layer depends on the distance from the interface. It was measured by scanning the interface with electron pencils [6], laser and acoustic probes [7,8]. More accurate results were obtained with the method of thermally stimulated depolarization [9]. For example, the double layer of the system poly(tetrafluoroethylene vinylidene fluoride) copolymer/steel has been characterized by the maximum width  $10^{-3}$  cm and the magnitude of the charge density which changes within the double layer from  $5 \times 10^{16}$   $\text{cm}^{-3}$  nearby the interface to  $5 \times 10^{13}$   $\text{cm}^{-3}$  on the border of the double layer (1–10  $\mu\text{m}$ ). These charge concentrations correspond to the electric field values  $10^7$ – $10^4$  V/cm.

Thus, we can suppose that sometimes in the interface region of the metal–polymer system the macromolecular

chains are under the influence of rather strong electric field of the metal–polymer double layer. When the influence of chemical and physico-chemical bonding on the stability of metal–polymer system is localized at the interface, the electric field of double layer may distribute its influence to a considerable distance into the bulk polymer. It can result in the changes of a number of physical characteristics of the coating. There are experimental evidences that dielectric properties of polymers are changed under the influence of the external electrical field of 2, 5–7 kV/cm [10], this value is comparable with the magnitude of the electric field along the border of the double layer mentioned earlier.

In this work we tried to apply the dielectric relaxation spectroscopic (DRS) technique in order to study the possible influence of the double layer on molecular motions in polyurethane (PU) on the dependence of the thickness of the polymer layer, substrate material and the presence of the adhesion interaction.

## 2. Experimental

Linear PU, used as a coating, was prepared from poly(oxy-propylene)diol of molecular weight 425 and hexamethylendiisocyanate. The solution of PU in tetrahydrofuran (5%) was used for the preparation of the coatings of

---

\* Corresponding author. Tel.: + 33-(0)2-4383-3266; fax: + 33-(0)2-4383-3518.

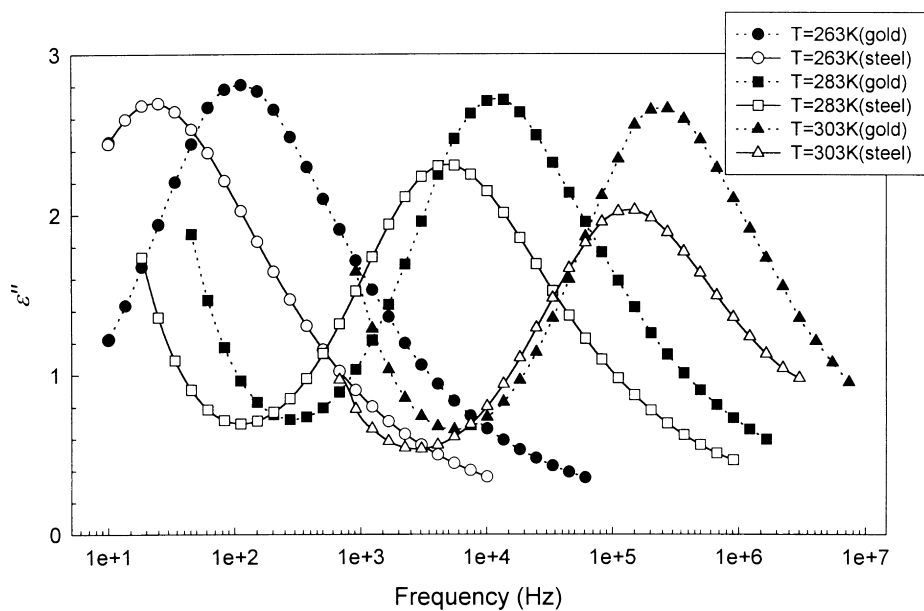


Fig. 1. DRS spectra of the PU for the M-PU-M system, thickness of the PU layer 10  $\mu\text{m}$ .

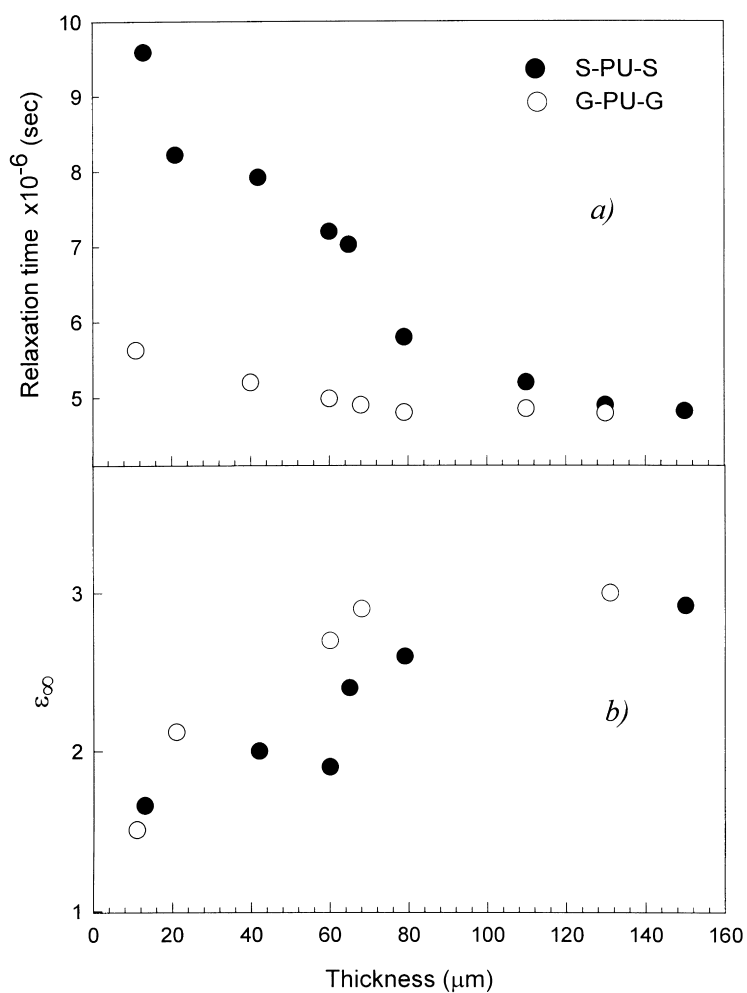


Fig. 2. Dependence of : (a) the  $\alpha$ -relaxation time; (b)  $\epsilon_{\infty}$  on the thickness of the PU layer at 273 K.

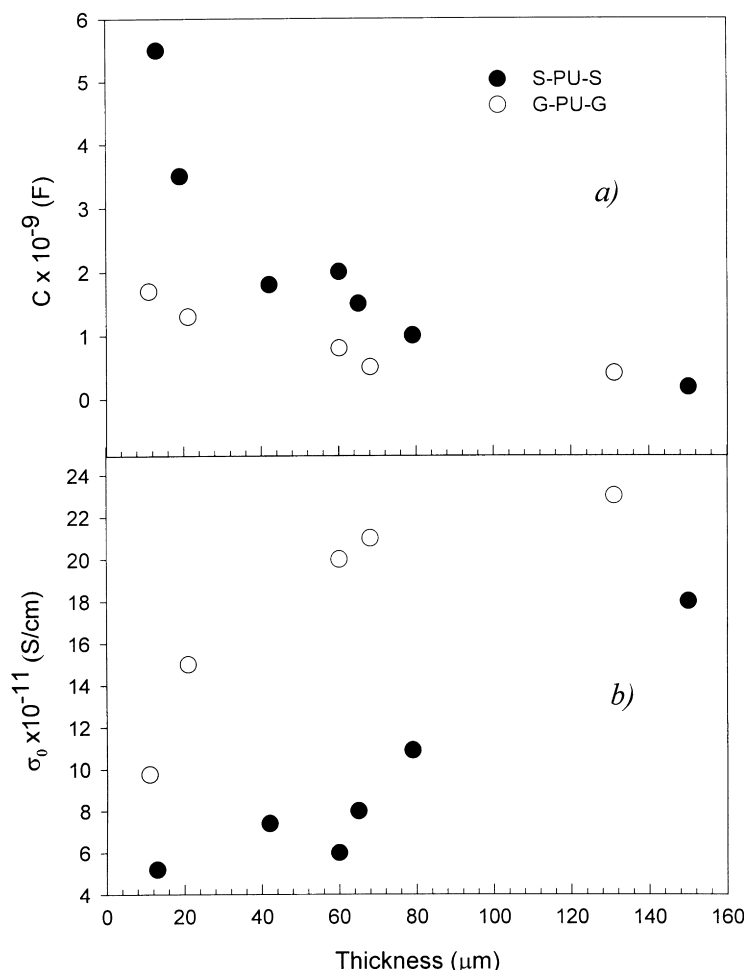


Fig. 3. Dependence of: (a) the capacitance; (b) DC conductivity on the thickness of the PU layer at 273 K.

different thickness (10–150 μm) on steel or gold substrates. The disk sample geometry was used for the DRS measurements: the sample material placed into a sample cell consisting of two parallel capacitor plates (diameter 40 mm). In order to have the adhesion contact of the PU layer with both the electrode surfaces, the coated electrodes were joined together by coated sides after 24 h exposition at 60°C in a vacuum box. When the polymer became viscous after heating, the electrodes containing the sample were pressed between two parallel plates using guard spacers in order to reach needed sample thickness. After cooling, the

thickness was measured by digimatic micrometer with an accuracy of 1 μm. For the measurement samples with a minimum difference of thickness ±3 μm were taken. The sample cell with adhesion contact at only one electrode is also used. In this case, the PU layer is not adhered to the second electrode. Before covering, the gold electrodes were carefully washed in ethanol, the steel electrodes were additionally polished with diamond powder on a porous paper.

DRS measurements were made with Broadband Dielectric Spectrometer (Novocontrol GmbH) in the frequency range 0.1 Hz–10 MHz at temperatures from –120 to 50°C, the temperature was controlled by a temperature controller (Quatro, Novocontrol), using a gas stream of nitrogen, with an accuracy of ±0.1°C.

In order to quantify the mean relaxation time in the range of the present interest the frequency domain impedance analysis is the method of choice. As a function of sample temperature we obtain the complex dielectric function:

$$\epsilon^*(\omega) = \epsilon'(\omega) - i\epsilon''(\omega).$$

Experimental dielectric spectrum  $\epsilon''(\omega)$  is fitted by the Havriliak–Negami (HN) function [11] and an optional

Table 1

$S_{\text{diff}}$  and  $R_a$  data for the steel and gold electrode surfaces estimated on the area 0.7; 7 and 70 μm<sup>2</sup>

Electrode	Tested space (μm <sup>2</sup> )	$R_a$ (nm <sup>2</sup> )	$S_{\text{diff}}$ (%)
Steel	0.7	5 ± 1	1.7
	7	30 ± 2	1
	70	55 ± 3	0.75
Gold	0.7	3 ± 1	1.7
	7	19 ± 2	1.9
	70	105 ± 3	0.6

conductivity term as shown later:

$$\epsilon^*(\omega) = \epsilon_\infty + \sigma_0 \omega^N + \frac{\Delta\epsilon}{(1 + (i\omega/\omega_0)^\alpha)^\beta},$$

where  $\omega = 2\pi f$ ;  $\epsilon_\infty$  denotes the vacuum permittivity;  $\sigma_0$  the DC conductivity;  $N$  the exponential factor, in most cases is equal to 1;  $\Delta\epsilon$  is the difference between the low and high frequency limits of  $\epsilon'$  over the relaxation to which the HN function applies,  $\Delta\epsilon$  is also proportional to the area below the  $\epsilon''$  relaxation peak;  $\epsilon_\infty$  is the unrelaxed value of permittivity;  $\alpha$  and  $\beta$ -shape parameters. Fitting of the experimental dielectric spectra  $\epsilon^*(\omega)$  were made with WinFit 2.4 (1996) software of Novocontrol GmbH [12].

The surfaces of both gold and steel electrodes were investigated by atomic force microscopy (AFM). Topography of the surfaces was evaluated by Nanoscop III, digital instruments. To judge the roughness, the values of mean roughness ( $R_a$ ) and surface area ratio ( $S_{\text{diff}}$ ) were evaluated.  $R_a$  is the mean value of the surface relative to the central plane and is calculated using:

$$R_a = \frac{1}{L_x L_y} \int_0^{L_y} \int_0^{L_x} |f(x, y)| dx dy,$$

where  $f(x, y)$  is the surface relative to the central plane and  $L_x$  and  $L_y$  are the dimensions of the surface.  $S_{\text{diff}}$  is the percentage of the three-dimensional surface area to the two-dimensional surface area produced by projecting surface onto the threshold plane:

$$S_{\text{diff}} = \left[ \frac{\sum(\text{surface area})_i}{\sum(\text{projected area})_i} - 1 \right] \times 100\%.$$

### 3. Results and discussion

Four types of the dielectric relaxation are common for PUs [13,14]:  $\alpha$  (cooperative motions)  $\beta$  and  $\gamma$  (local motions), and MWS (Maxwell–Wagner–Sillars) or interfacial polarization effect.

The  $\alpha$  relaxation is associated with glass–rubber transition. The glass-transition temperature  $T_g$  is usually taken as the temperature at which the  $\alpha$ -relaxation peak in the dielectric spectrum is at 0.01 Hz ( $T_\alpha$ ) [15–17]. Usually, in TSDC measurements for the glass transition band the electrode material and polymer thickness play a considerable role [9,18] and the origins of this influence has not been clearly defined. The evolution of the  $\alpha$ -relaxation peak with temperature for the PU is shown in Fig. 1. As compared to the gold electrodes, for the steel ones this peak shifts to lower frequencies and are of less intensity. Using HN fit data the dependencies of the relaxation time ( $\tau_\alpha$ ) and  $\epsilon_\infty$  on the thickness are obtained (Fig. 2 (a) and (b), is an example taken at 293 K). Besides, the values of capacitance ( $C$ ) and  $\sigma_0$  for the samples with different thickness of the PU layer are obtained at 1 kHz (Fig. 3 (a) and (b)). Each data point represents an averaged value from three experiments.

From Fig. 2(a), we can see a rising of the  $\tau_\alpha$  for the steel electrodes, when the thickness of the PU decreases starting from 60  $\mu\text{m}$ . In the case of gold–PU–gold (G–PU–G) system we can notice the increasing of the  $\tau_\alpha$  at smaller thickness, but not so significant than for steel–PU–steel (S–PU–S) system. The capacitance-thickness dependencies (Fig. 3(a)) shows a similar character. On contrary, the values of the permittivity of the PU at infinite frequency and of the specific resistance decrease with the thickness. Particularly, for the S–PU–S system the values of both  $\epsilon_\infty$  and  $\sigma_0$  are smaller than for the G–PU–G system. Hence, we can say that the macromolecular segments become less flexible when the PU layer between the electrodes decreases. This effect is much more pronounced for the steel electrodes.

To discuss the influence of the electrode material on the properties metal–polymer interface it is very important to resolve the following methodical question. We make the measurements of thin polymer layer (starting from 10  $\mu\text{m}$ ) between two electrodes. In this case the roughness can play a role. As we can see from  $S_{\text{diff}}$  and  $R_a$  data obtained by means of AFM (Table 1) there is no considerable difference between the surfaces of gold and steel electrodes. For the gold electrode  $R_a$  is less than that for the steel one at the same  $S_{\text{diff}}$  value, so that the gold electrode surface has higher fractal dimensions than the steel one. As compared to the polymer thickness ( $10 \pm 3 \mu\text{m}$ ) and the expected maximum width of the metal–polymer electric double layer (1–10  $\mu\text{m}$ ), the local roughness 2–7 nm (for the area 0.7  $\mu\text{m}$ ) is much smaller. Thus, the contribution of chemically transformed polymer fragments at the interface on the dielectric relaxation properties of the polymer can hardly be expected.

It is important to notice that with the decreasing thickness of PU layers the values of  $\epsilon_\infty$  and  $\sigma_0$  decrease; for the S–PU–S system, this is more significant. As a rule, the concentration of the charge carriers should increase in thin layer, specially for the steel–PU interface [9], giving rise to conductivity and dielectric loss. We suppose that, in this case, for the symmetrical system with the adhesion contacts on both sides of the PU film, an interaction of the electric fields of the same polarity in the middle of the polymer layer can shield the charge transfer between two electrodes. This explanation has been given for the TSDC data obtained for the nonohmic contact in the metal/polyparaphenylene/metal system [18]. Similar effect was observed for the thermally stimulated relaxation of the potential in Teflon films [19]. Therefore, we find it very fruitful to consider two systems: both side and one side adhesion layer, we shall mark it M–PU–M and M–PU|M, respectively.

$\alpha$ -relaxation parameters were obtained by fitting the dielectric spectra with HN function, and the activation energy of the relaxation process was calculated using Vogel–Fulcher–Tamman–Hesse equation [20–22]:

$$\tau(T) = \tau_0 \exp \left[ \frac{E_a}{k_b(T - T_V)} \right],$$

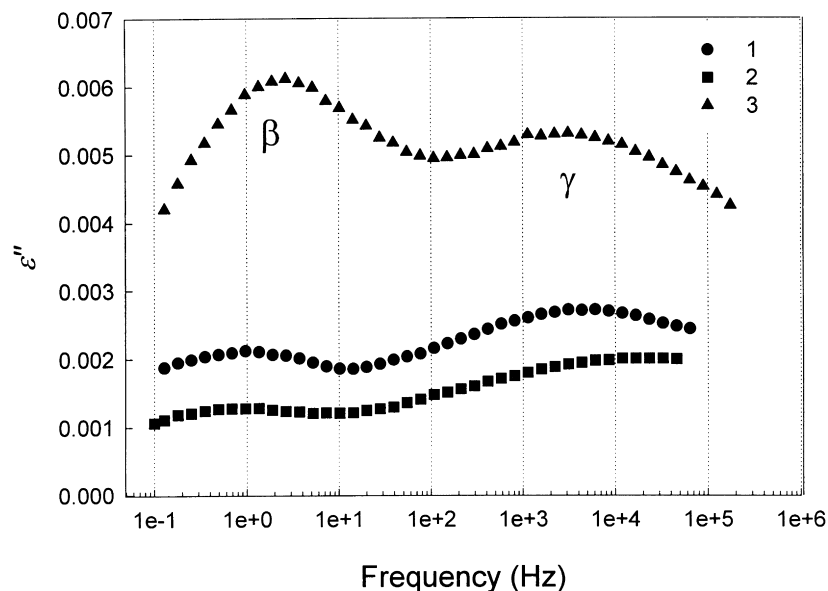


Fig. 4. DRS spectra of the PU at 193 K: (1) G–PU–G, thickness 10  $\mu\text{m}$ ; (2) S–PU–S, thickness 10  $\mu\text{m}$ ; (3) G–PU–G, thickness 70  $\mu\text{m}$ .

where  $E_a$  is constant being related to the activation energy,  $\tau_0$  is the relaxation time at infinite temperature,  $k_b$  is Boltzmann constant and  $T_V$  is the Vogel Fulcher temperature ( $T$  at infinite relaxation time). Fitted data of the  $\alpha$ -relaxation are presented in Table 2. We can see, that dielectric relaxation characteristics depend not only on the thickness of the PU layer and electrode material, but on presence of the adhesion contact with the second electrode as well. For the S–PU–S system the increasing of the relaxation time and  $E_a$  is more considerable, and the characteristics of dielectric loss ( $\Delta\epsilon$  and  $\epsilon_\infty$ ) and specific conductivity have smaller values, as compared to S–PU|S system. For the gold electrodes difference of the relaxation characteristics with the thickness of the PU and between the two electrode systems is relatively small. Very low values of  $\Delta\epsilon$ ,  $\epsilon_\infty$ , and  $\sigma_0$  for G–PU|G system are probably connected with very small interface interaction in the case of non-adhesion contact of the gold and PU surface. Changes of the shape parameters of the  $\alpha$ -relaxation band ( $\alpha$  and  $\beta$ ) are not considerable.

The  $\gamma$  and  $\beta$ -relaxation correspond to the local motions in the glassy state polymer [15,16]. The dielectric relaxation spectra for the PU used by us which illustrate the  $\gamma$  and  $\beta$  peaks are shown in Fig. 4. The mechanisms of these relaxation processes are not systematically studied [14]. The  $\gamma$  mechanism is associated with motions of  $(-\text{CH}_2-)_n$  units [16,13] whereas in the  $\beta$  mechanism the polar groups are probably involved [14,16]. There is a strong dependence of the  $\beta$  peak on water content in the PU, but it does not completely disappear in dried samples. According to Illers [24] this mechanism can be connected with the motions of the carbonyl groups to which water molecules are attached by hydrogen bonds, but there are other interpretations [14,16]. In our case, there is a strong dependence of the

relaxation time and the intensity of the  $\gamma$  and  $\beta$  peaks on thickness and electrode material (Table 3). The Arrhenius plots for the  $\beta$ - and  $\gamma$ -relaxation were fitted by the Arrhenius equation, to obtain  $E_a$ :

$$\ln(\tau) = \ln(\tau_0) + \frac{E_a}{k_b T}.$$

From Table 3, we can see that  $\beta$ -relaxation time and  $\Delta\epsilon$  are strongly dependent on the thickness and the electrode system, and in spite of this difference,  $E_a$  is practically the same in all cases. The parameter  $\alpha$  is less for the steel electrodes and decreases with the thickness of the PU layer (parameter  $\beta$  depends on the position of the  $\gamma$ -relaxation band). Thus, the  $\beta$ -relaxation band is more broad and less intense (according to  $\Delta\epsilon$ ) when the thickness of the PU layer is less and steel electrodes being used. We can try to consider our data in the frames of the conception [24] according to which the  $\beta$ -relaxation is associated with local motions of C=O groups bonded with adsorbed water. In our case for the equal exposition time of the samples in the vacuum at 60°C, removing of the water is more considerable for the small thickness. Besides, the substrate material probably plays a role in holding back the adsorbed water. As in the case of S–PU–S system, the value of the relaxation strength ( $\Delta\epsilon$ ) is smaller than for G–PU–G one (Table 3). It can mean that in the case of the steel substrate, water is easily removed from the thin PU film. The S–PU|S system in comparison with G–PU|G one displays a more pronounced relaxation strength. In this case, the influence of humidity on the noncovered electrode can be significant. Unfortunately, we are not able to give more detailed explanation of the interface influence on  $\beta$ -relaxation because of the lack of knowledge about the nature of this relaxation in PUs.

Table 2  
The  $\alpha$ -relaxation properties of the PU in the dependence on the electrode system

Electrode system	Thickness of the PU, $\mu\text{m}$	$\tau$ (s) (at 273 K)	$\Delta\epsilon$ (at 273 K)	$\alpha$ (at 273 K)	$\beta$ (at 273 K)	$\epsilon_{\infty}$ (at 273 K)	$\sigma_0$ , S/cm (at 273 K)	$E_{\text{tr}}$ , eV	$\tau_0$ (s)	$T_V$ , K
S-PU-S	10	$6.373 \times 10^{-4}$	0.376	0.822	0.454	0.320	$5.167 \times 10^{-14}$	0.157	$7.695 \times 10^{-14}$	188.6
	40	$3.479 \times 10^{-4}$	4.137	0.797	0.493	2.352	$2.255 \times 10^{-12}$	0.140	$1.022 \times 10^{-12}$	190.5
G-PU-G	10	$2.942 \times 10^{-4}$	0.531	0.817	0.450	0.388	$8.600 \times 10^{-14}$	0.120	$9.906 \times 10^{-13}$	198.9
	40	$2.174 \times 10^{-4}$	8.745	0.795	0.590	3.257	$6.009 \times 10^{-12}$	0.111	$2.645 \times 10^{-12}$	198.9
S-PU S	10	$2.903 \times 10^{-4}$	2.987	0.823	0.496	1.436	$7.925 \times 10^{-13}$	0.130	$2.214 \times 10^{-12}$	187.0
	40	$2.345 \times 10^{-4}$	12.81	0.818	0.564	4.118	$7.787 \times 10^{-12}$	0.122	$1.505 \times 10^{-12}$	195.8
G-PU G	10	$1.988 \times 10^{-4}$	0.196	0.807	0.362	0.291	$9.661 \times 10^{-14}$	0.120	$8.801 \times 10^{-11}$	196.2
	40	$2.010 \times 10^{-4}$	0.934	0.827	0.371	0.964	$3.546 \times 10^{-13}$	0.109	$2.815 \times 10^{-12}$	198.9

Table 3  
The parameters of the  $\beta$ - and  $\gamma$ -relaxation in the dependence on the electrode system

Electrode system	Thickness of the PU, $\mu\text{m}$	$\beta$ -relaxation				$\gamma$ -relaxation					
		$\tau$ , (s) (at 193 K)	$\Delta\epsilon$ (at 193 K)	$\alpha$ (at 193 K)	$\beta$ (at 193 K)	$E_{\text{tr}}$ , eV	$\tau$ , (s) (at 193 K)	$\Delta\epsilon$ (at 193 K)	$\alpha$ (at 193 K)	$\beta$ (at 193 K)	$E_{\text{tr}}$ , eV
S-PU-S	10	0.10	$3.91 \times 10^{-3}$	0.51	1	0.52	$3.35 \times 10^{-6}$	$1.96 \times 10^{-2}$	0.28	1	0.564
	40	0.41	$1.86 \times 10^{-2}$	0.85	0.88	0.52	$5.73 \times 10^{-5}$	$1.56 \times 10^{-2}$	0.54	0.72	0.962
S-PU S	10	0.040	$4.05 \times 10^{-2}$	0.50	0.92	0.57	$5.51 \times 10^{-5}$	$1.04 \times 10^{-1}$	0.39	0.52	0.363
	40	0.022	$2.65 \times 10^{-1}$	0.40	1	0.58	$9.44 \times 10^{-5}$	$3.58 \times 10^{-1}$	0.56	0.82	0.329
G-PU G	10	1.010	$7.20 \times 10^{-3}$	0.63	0.85	0.57	$1.06 \times 10^{-4}$	$7.20 \times 10^{-3}$	0.35	0.66	0.639
	40	0.045	$2.98 \times 10^{-2}$	0.46	1	0.58	$9.03 \times 10^{-5}$	$4.99 \times 10^{-2}$	0.48	0.74	0.425

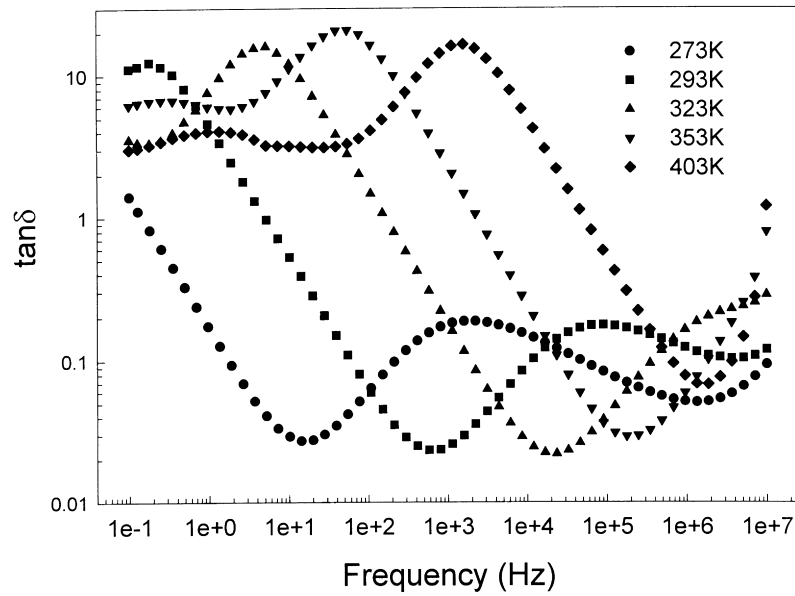


Fig. 5. DRS spectra in  $\tan \delta$  representation of the S-PU-S system, thickness of the PU layer 10  $\mu\text{m}$ .

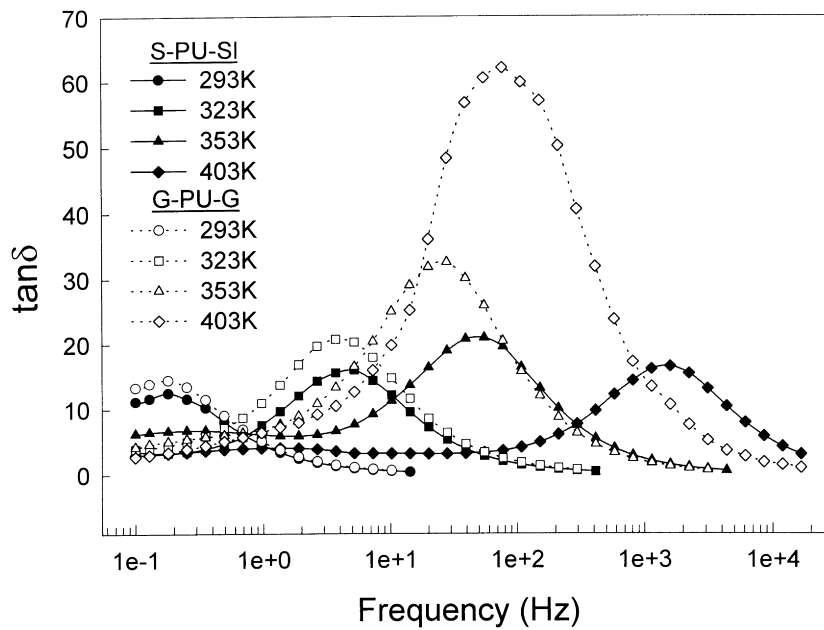


Fig. 6. DRS spectra in  $\tan \delta$  representation, thickness of the PU layer 10  $\mu\text{m}$ . The lines are to guide the eye.

Table 4  
The parameters of the MWS relaxation of the PU (thickness 10  $\mu\text{m}$ ) between steel and gold electrodes

Electrode system	$\tau$ .(s) (at 363 K)	$\Delta\epsilon$ (at 363 K)	$\alpha$ (at 363 K)	$\beta$ (at 363 K)	$\sigma_0$ , $\Omega$ cm	$E_a$ , eV
S-PU-S	0.14	$3.8 \times 10^{+3}$	1	1	$2.74 \times 10^{+8}$	0.17
G-PU-G	0.43	$8.2 \times 10^{+4}$	1	1	$2.93 \times 10^{+8}$	0.23

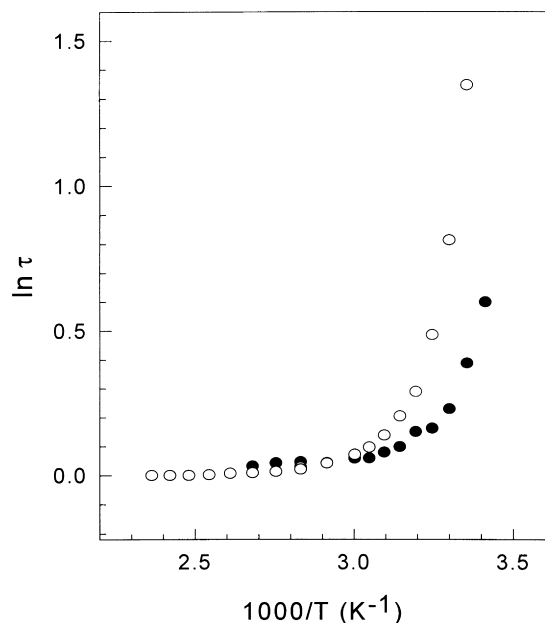


Fig. 7. Arrhenius plots for MWS relaxation of the PU between gold (●) and steel (○) electrodes, thickness of the PU layer 10  $\mu\text{m}$ .

For the  $\gamma$ -relaxation process the relaxation parameters and  $E_a$  as well are strongly dependent on the thickness of the PU layer and the electrode system. In comparison with  $\alpha$  or  $\beta$ -relaxation, for the  $\gamma$ -relaxation the magnitude of  $E_a$  is lower in the cases of the steel electrodes, M-PU|M electrode systems, and for the more thick PU layer. It is hard to give an appropriate explanation for the behavior of the  $\gamma$ -relaxation in the terms of the conception [15,23], where  $\gamma$ -relaxation mechanism is connected with the motions of  $(-\text{CH}_2-)_n$  groups. We have to take into account that the PU we use contains oxybutanol groups  $-\text{O}-\text{CH}_2-\text{CH}(\text{CH}_3)-$ . In this case the interaction of the ether oxygen with electric field of the double layer can be suspected.

Usually, the  $\alpha$ -relaxation is accompanied with the MWS relaxation process [25]. The latter was described for PUs as related to ionic polarization in the diffuse interface boundary region between hard and soft segment phase, based on the DRS and TSDC measurements [14,26,27]. On the  $\epsilon''$ -frequency dependence the MWS relaxation is related to an increase of permittivity in low frequency region. Presenting the data in the  $\tan \delta$  formalism (Fig. 5) the peak of the MWS dielectric loss becomes better defined and suitable for fitting. As we can see in Fig. 6, the MWS relaxation depends on the electrode material, in the case of steel the intensity is less and with heating, the shift in high frequency region is more pronounced. Moreover, we can see the appearance of a second peak at temperatures higher than 323 K (Figs. 5 and 6), which is less intensive than the first one, but which is absent in the case of the gold electrodes.

The HN function was also applied to obtain the parameters of the MWS relaxation, presented in  $\tan \delta$  formalism. From Arrhenius plots (Fig. 7) we can see, that the

MWS relaxation has a transition point. At temperatures above this point the plot can be considered linear and can be fitted by Arrhenius equation. From the Table 4 we can see, that it is practically Debye process ( $\alpha = \beta = 1$ ), in the case of the steel electrodes the relaxation time and  $E_a$  are less than for the gold electrodes. This fact probably certifies that the polarized layer of the PU at the interface forms easily at the steel substrate. The smaller values of  $\Delta\epsilon$  and specific resistance for the S-PU-S system can testify to the shielding effect of the PU-M interface layers for the charge transfer, as it is supposed earlier. The appearance of the second band for the S-PU-S system also presents the particularities of the influence of the steel/PU interface, but its origin and mechanism are outside of this work.

#### 4. Conclusions

As a result of the strong interfacial interaction of the PU with the steel substrate, macromolecules are under the influence of the electric field of the metal-polymer double layer. This influence becomes more considerable for the small thickness of the PU layer ( $< 60 \mu\text{m}$ ) and is manifested in the changes of the dielectric relaxation characteristics:  $\alpha$ -relaxation time and activation energy increase as compared to the gold electrodes, local  $\beta$ - and  $\gamma$ -relaxation mechanisms also change. In the case of adhesion interaction of the PU with both the electrodes the effect of double layer is more pronounced. In this case the shielding effect for the DC conductivity is observed. For the steel electrodes the peak of dielectric relaxation associated with interfacial polarization appears at lower temperatures as compared to the gold electrodes.

#### Acknowledgements

The authors thank Prof. P. Pissis (Athens, Greece) for useful discussion, F.Paris and D.Ausserre (Université du Maine) for providing AFM measurements and La Région des Pays de la Loire for the financial support.

#### References

- [1] Garbassi F, Morra M, Occhiello E. Polymer surfaces. From physics to technology. NY, USA: Wiley, 1994.
- [2] Derjaguin VB. Research 1955;8:70–363.
- [3] Derjaguin VB, Krotova NA, Smigla VP. Adgasion of solids Nauka, Moscow, 1977.
- [4] Derjaguin VB, Kluev VA, Anisimova VJ, Toporov Y P, Krotova NA. Colloid and Interface Sci. 1980;77:472.
- [5] Hays DA. Fundamentals of Adhesion. New York: Plenum Press, 1991 p. 249.
- [6] Possart W, Röder A. Phys Stat Sol 1984;84:319.
- [7] Anderson RA, Kurtz SR. J Appl Phys 1984;56:2856.
- [8] Sessler GM, West JE, Gerhard G. Phys Res Lett 1982;48:563.
- [9] Lipson AG, Kuznetsova EV, Sakov DM, Toporov Yu P. Poverhnost; Phisika, Khimiya, Mekhanika 1992;12:74.



- [10] Tokoro T, Thoyama K, Nago M, Kosaki M. Proc of 5th Conf on Conduction and Breakdown in Solid Dielectrics. IEEE 1995, 426.
- [11] Havriliak S, Negami S. J Polym Sci Polym Symp 1966;14:89.
- [12] Schaumburg G. Dielectric Newsletter 1996;:4.
- [13] Spathis G, Kontou E, Kevalas V, Apekis L, Christodoulides C, Pisis P, Olivon M, Quinquenet S. J Macromol Sci Phys 1990;B29:31.
- [14] Pisis P, Apekis L, Christodoulides C, Niaonakis M, Kritsis A, Nedbal J. J Polym Sci B: Polym Physics 1996;34:1529.
- [15] Hedvig P. Dielectric spectroscopy of polymers. Bristol: Adam Hilger, 1977.
- [16] McCrum NG, Read BE, Williams G. Inelastic and dielectric effects in polymer solids. London and New York: Wiley, 1967.
- [17] Nagai KL. Macromolecules 1991;24:4865.
- [18] Ettaik H. Etude des couches minces de polyparaphénylene et de l'interface métal-polymère par des méthodes électriques et physico-chimiques, PhD thesis, Université de Nantes, France 1992.
- [19] Boitsov VG, Rychkov AA. Sov Phys Tech Phys 1985;30(5):526.
- [20] Vogel H. Phys Z 1921;22:645.
- [21] Fulcher GS. J. Am Ceram Soc 1925;8:339.
- [22] Tamman G, Hesse WZ. Anorg Allg Chem 1926;156:245.
- [23] Jacobs H, Jenckel E. Macromol Chem 1961;47:72.
- [24] Illers KH. Macromol Chem 1960;38:168.
- [25] Hanai T. In: Sherman P, editor. Emulsion science, London: Academic Press, 1968. pp. 353.
- [26] Pisis P, Apekis L. J Non Crist Solids 1991;131–133:1174.
- [27] Pisis P, Kanapitsas A, Savelyev YV, Akhranovich ER, Privalko EG, Privalko VP. Polymer 1998;39:3431.